**METEOR (BARRINGER) IMPACT CRATER, AZ, USA: INDICATIONS FOR RAMPART-LIKE EJECTA MORPHOLOGIES?** G. Wulf[1] and T. Kenkmann[1], [1]Institute of Earth and Environmental Sciences - Geology-, Albert-Ludwigs-University Freiburg, Germany, gerwin.wulf@geologie.uni-freiburg.de.

**Introduction:** The Meteor crater in northern Arizona is one of the youngest and best-preserved terrestrial impact craters. The approximately 50 kyr old impact crater is a simple crater with a crater diameter of 1.2 km and a pronounced crater rim of 40-50 m [1-4]. The crater structure shows a square shape caused by two mutually perpendicular sets of vertical joints [e.g. 1, 5]. The well-preserved proximal ejecta blanket of Meteor Crater is composed of an inverted sequence of Coconino, Toroweap, Kaibab, and Moenkopi strata [1, 2, 6]. The Meteor Crater Sample Collection makes geologic samples from the Meteor Crater ejecta blanket available that were obtained during the 1970's [6]. The data allow extensive digital analyses of the geologic data using latest and advanced computer techniques. Here we present preliminary results showing the interpolation and reconstruction of the morphology of the ejecta blanket of the crater as well as the structural uplift of the crater rim and the paleo-surface.

**Methods:** We followed the routine developed and applied for the reconstruction of the Ries crater ejecta blanket described in detail in Sturm et al. 2013. We used extracted mapping information of the autochthonous-allochthonous ("ejecta base") intersections from the geologic map of Meteor Crater [7], and descriptions of 147 drillings made available by the Meteor Crater Sample Collection to interpolate the morphology and thickness variation of the ejected material outside the crater. In addition, we included elevation data of the present-day weathered surface of the ejecta to obtain minimum thickness estimations in regions outside the crater. Therefore, a digital elevation model with 1 m resolution (collected by M. Palucis through the NSF-sponsored National Center for Airborne Laser Mapping (NCALM)) and geologic information were combined in ArcGIS 10.4 by ESRI. To derive the paleo-surface we used the autochthonous-allochthonous intersections of the drillings in distances larger than 1.7 crater radii from the crater center to exclude structurally uplifted target rocks. In the following steps, ArcGIS was used to build interpolation data between elevation points for further reconstruction of the paleo-surface, the structurally uplifted target rocks ("ejecta base") and the ejecta top (Figs. 1, 2). For the ejecta base and top, the spline interpolation method delivered the best results in terms of geologic interpretation.

For morphometric comparisons, we determined the mean elevation of the interpolated paleo-surface, structural uplift/ ejecta base and weathered surface of the ejecta at defined radial distances from crater rim (bins of 10 m) in order to construct averaged radial elevation profiles (Fig. 3).

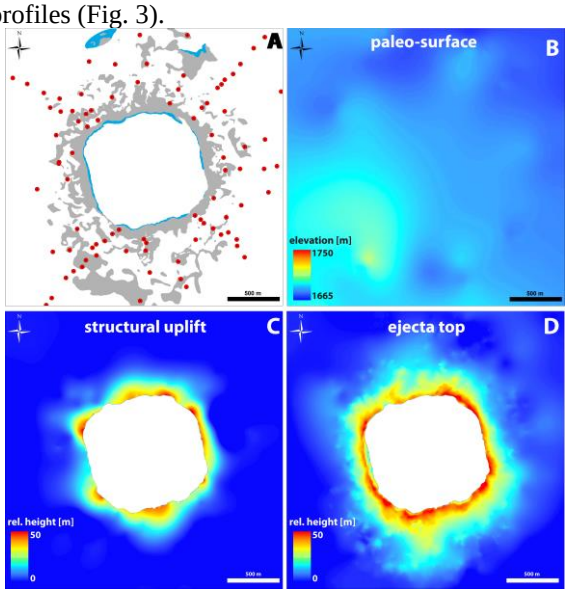


Fig.1: Base data for the interpolation (A; red = drillings with contact between ejecta and Triassic Moenkopi, blue = Triassic Moenkopi, grey = ejected material). The interpolation results of the paleo-surface (B) in comparison to the interpolated structural uplift (C) and the weathered surface of the ejecta (D) (C and D are displayed in relative heights to the paleo-surface).

**Results and Discussion:** The interpolated paleo-surface shows a relatively flat terrain with only minor scattered hills or ridges (Fig. 1b). A regional trend from NE to SW is recognizable with higher elevation values in the SW (~7 m/ 1000 m), similar to older studies [6]. The difference between the paleo-surface and the interpolated autochthonous-allochthonous boundary ("ejecta base"), defined by the contact between ejected material and the Triassic Moenkopi formation (Tm), can be used to estimate the extent of the structural uplift (Fig. 1c). The mean structural uplift at the crater rim is approximately 35 m (maximum of 52 m) and is detectable to a distance of ~340 m from the crater rim or 1.56 crater radii from the crater center (Figs. 1c, 3).

The difference between the present-day weathered surface of the ejecta and the paleo-surface can be used to quantify the overall volume above the paleo-surface and the ratio of ejected material to structurally uplifted

target rocks (Figs. 1c, 3). It is possible to obtain a minimum thickness estimation of the ejecta blanket and the ejecta distribution by considering the ejecta base (Fig. 2). Interestingly, the ejecta is not evenly distributed around the impact crater.

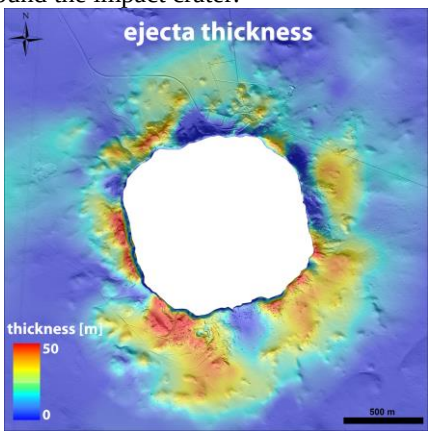


Fig.2: Interpolated ejecta thickness distribution.

The ejecta is significantly thicker in the southern part. In addition, the ejecta thickness distribution deviates distinctly from a steady decrease with radial range, as seen for lunar craters [8]. In contrast, the ejecta at some parts of the crater rim appears to be thinned out or highly eroded whereas the ejecta thickness shows local highs in a distance of 300-600 m from the crater rim (Fig. 2). To take the fact into account that the interpolated ejecta thickness bases upon the present-day weathered surface of the ejecta it makes sense to consider the maximum ejecta thickness, and thus the least eroded parts. Therefore, a radial elevation profile of the maximum ejecta values at defined radial distances from crater center (bins of 10 m) was derived in addition to the ejecta mean values. The maximum ejecta distribution shows exceptionally high values in a distance of 300-600 m from the crater rim (or 1.5-2.0 crater radii from crater center) (Fig. 3).

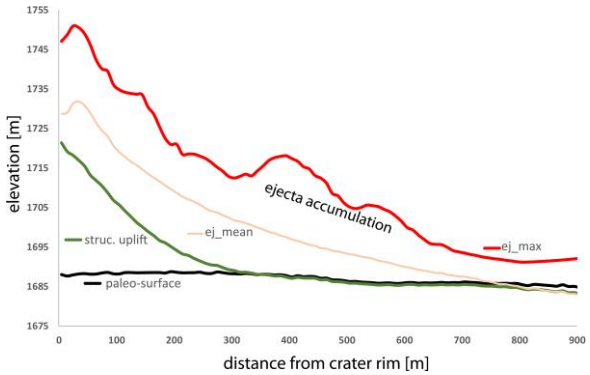


Fig.3: Averaged radial elevation profiles of the interpolated paleo-surface, structural uplift/ ejecta base and weathered surface of the ejecta.

Different explanations are conceivable for the uneven ejecta distribution and ejecta accumulation. The higher ejecta thicknesses in the southern part could be due to an oblique impact from NNW building thicker deposits in downrange direction, as postulated by Poelchau et al. 2009 [5]. The ejecta thickness profile shows similarities to rampart-like ejecta morphologies of Martian and some terrestrial impact craters that show accumulation of ejecta in distal parts [9-11]. Possibly, the wetter climate conditions during the Wisconsin period [12] allowed the formation of a weakly pronounced but detectable rampart, at least in the southern part. Interestingly, recent studies of the Meteor Crater Sample Collection indicate more complex crater excavation and ejecta emplacement processes for the distal ejecta parts, with mixed facies better described as “chaotic” deposits [13, 14].

**Conclusions and Outlook:** The ejecta thickness distribution beyond the crater rim of Meteor crater shows significantly higher values in the southern part and similarities to rampart-like ejecta morphologies. Therefore, we suggest that Meteor crater shows a weakly pronounced but detectable eroded remnant of a small ejecta rampart, at least in the southern part. In future works, the interpolation methods will be improved and it will be proven in more detail if the ejecta accumulation is due to rampart formation processes or erosional processes of the crater rim and slope.

**Acknowledgements:** We thank Tenielle Gaither for making the data of the *Meteor Crater Sample Collection* https://astrogeology.usgs.gov/facilities/meteor-crater-sample-collection available. In addition, we want to thank David A. Kring for offering a multitude of information and data in the course of the *Guidebook to the Geology of Barringer Meteorite Crater* [12].

**References:** [1] Shoemaker E. M. (1963) *The moon, meteorites and comets*. pp. 301–336. [2] Shoemaker E. M. and Kieffer S.W. (1974) *Guide-book to the geology of Meteor Crater*, pp. 66. [3] Nishiizumi K. et al. (1991) *Geochim. Cosmochim. Acta*, *55*, 2699. [4] Phillips F. M. et al. (1991) *Geochim. Cosmochim. Acta*, *55*, 2695. [5] Poelchau M. H. et al. (2009) *JGR* vol. 114(E1):E01006. [6] Roddy D. J. et al. (1975) *Proc., 6th Lunar Sci. Con*. pp. 2621–2644. [7] Shoemaker E.M. (1960) *Impact mechanics at Meteor Crater Arizona*: unpubl. PhD Thesis, Princeton 55 pp. [8] McGetchin T.R. et al. (1973) *EPSL*, vol. 20, pp. 226–236. [9] Sturm S. et al. (2013) *Geology*, vol. 41(5), pp. 531-534. [10] Wulf G. and Kenkmann T. (2015) *MAPS*, vol. 50, pp. 173–203. [11] Barlow N.G. et al. (2000) *JGR*, vol. 105, pp. 26,733–26,738. [12] Kring D. A. (2017) Guidebook to the Geology of Barringer Meteorite Crater, Arizona, https://www.lpi.usra.edu/publications/books/barringer_crater_guidebook/. [13] Gullikson et al. (2016) LPSC 47, abstract #1541. [14] Gaither et al. (2016) LPSC 47, abstract #2113.